Available online at www.sciencedirect.com
ScienceDirect
Journal of Solid State Chemistry 180 (2007) 733–741
JOURNAL OF SOLID STATE CHEMISTRY
www.elsevier.com/locate/jssc

Crystal chemistry of the G-phases in the {Ti, Zr, Hf}–Ni–Si systems

A. Grytsiv[a], Xing-Qiu Chen[a], P. Rogl[a,*], R. Podloucky[a], H. Schmidt[a], G. Giester[b], V. Pomjakushin[c]

[a]*Institute of Physical Chemistry, University of Vienna, A-1090 Wien, Währingerstr. 42, Austria*
[b]*Institute of Mineralogy and Crystallography, University of Vienna, A-1090 Wien, Althanstr. 14, Austria*
[c]*Laboratory for Neutron Scattering, ETH Zurich & Paul Scherrer Institut, CH-5232 Villigen PSI, Switzerland*

Received 11 August 2006; received in revised form 6 November 2006; accepted 29 November 2006
Available online 6 December 2006

Dedicated to Prof. Dr. Wolfgang Jeitschko on the occasion of his 70th birthday

Abstract

Ternary compounds $M_6Ni_{16}Si_7$ (M = Ti, Zr, Hf) have been investigated by X-ray powder/single crystal and neutron powder diffraction. Compounds with Zr and Hf crystallize in the ordered Th_6Mn_{23} type ($Mg_6Cu_{16}Si_7$-type, space group $Fm\bar{3}m$), whereas $Ti_6Ni_{16.7}Si_7$ contains an additional Ni atom partially occupying the 24*e* site (*M*2 site, $x = 0.4637,0,0$; occ. = 0.119) inside a Ti octahedron; Ti atoms occupy a split position. $Ti_6Ni_{16.7}Si_7$ represents a new variant of the filled Th_6Mn_{23} type structure. Ab initio calculations confirm the structural difference: additional Ni atoms favour the 24*e* site for $Ti_6Ni_{16.7}Si_7$, however, for the Zr and Hf-based compounds the unoccupied site renders an energetically lower ground state. Enthalpies of formation of $Ti_6Ni_{17}Si_7$, $Zr_6Ni_{16}Si_7$, and $Hf_6Ni_{16}Si_7$ were calculated to be −68.65, −74.78, and −78.59 kJ/(mol of atoms), respectively.

Keywords: Titanium nickel silicide; Zirconium nickel silicide; Hafnium nickel silicide; Crystal chemistry; Diffraction (X-ray/neutron powder and X-ray single crystal); Ab initio calculations; Site preferences

1. Introduction

Dependent on the group number of the T element, ternary Laves or G-phases are observed to enter three-phase equilibria with TiAl + Ti_2Al in technically interesting Ti–Al-based duplex alloys [1]. In our previous articles [1–7], we reported on the crystal chemistry and site preference in the so-called G-phases from ternary systems Ti–M–Al, where M is an element of the 8th group. In all cases, the crystal structure of these compounds was determined to be a filled variant of the Th_6Mn_{23} type (space group $Fm\bar{3}m$ or subgroup $F\bar{4}3m$). Despite of the comprehensive investigation of Al-based G-phases, detailed crystallographic data on Si containing G-phases are rather limited. This is particularly true for the G-phases $M_6Ni_{16}Si_7$ (M = Ti, Zr, Hf), although the appearance of a $TiNi_{\sim 2}Si$ G-phase in commercial high-temperature Fe–Cr–Ni-based alloys (A-286, containing $Ti_{<2}Mo_{<1.5}Mn_{<1.3}V_{<0.3}Al_{<0.2}Si_{<1}$ and about 0.04 mass% C) was denoted 50 years ago [8]. Forthcoming investigations [9–13] revealed the general formula $Ti_6Ni_{16}Si_7$ and assigned the Th_6Mn_{23} ($Mg_6Cu_{16}Si_7$)—structure type but data on atomic coordinates are absent. In this work, we elucidated the crystal structure of $M_6Ni_{16}Si_7$ compounds (M = Ti, Zr, Hf) employing X-ray single crystal and neutron powder diffraction as well as ab initio calculations.

2. Experimental details

As cast alloys $Ti_6Ni_{16}Si_7$, $Zr_6Ni_{16}Si_7$ and $Hf_6Ni_{16}Si_7$ with a weight of 10–15 g each were prepared by argon arc melting (weight losses less than 0.1 mass%) on a water cooled copper hearth in Ti gettered argon from elemental ingots with minimal purity of 99.9 mass%. Single crystals of $Ti_6Ni_{16}Si_7$ were mechanically isolated from the crushed as cast alloy. Inspection on an AXS GADDS texture goniometer assured high crystal quality, unit cell dimensions and Laue symmetry of the specimens prior to

*Corresponding author. Fax: +43 1 4277 95245.
E-mail address: peter.franz.rogl@univie.ac.at (P. Rogl).

0022-4596/$ - see front matter © 2006 Elsevier Inc. All rights reserved.
doi:10.1016/j.jssc.2006.11.031

X-ray intensity data collection on a four circle Nonius Kappa diffractometer equipped with a CCD area detector employing graphite monochromated Mo$K\alpha$ radiation ($\lambda = 0.071073$ nm). Orientation matrix and unit cell parameters for a cubic system were derived using the program DENZO [14]. No absorption corrections were necessary because of the rather regular crystal shape and small dimensions of the investigated specimen ($30 \times 27 \times 30\,\mu m^3$). The structures were refined with the aid of the SHELXL-97 program [15].

X-ray powder diffraction data from as cast alloys were collected employing a Guinier Huber image plate system with Cu$K\alpha_1$ radiation ($8^\circ < 2\theta < 100$). Precise lattice parameters were calculated by least squares fits to the indexed 4θ values employing Ge as internal standard ($a_{Ge} = 0.5657906$ nm). For neutron powder diffraction as cast samples $Ti_6Ni_{16}Si_7$ and $Hf_6Ni_{16}Si_7$ were powdered to a grain size below 40 μm in order to reduce preferential orientation effects. Neutron diffraction was performed at room temperature on the high resolution HRPT diffractometer [16] at the SINQ spallation source of the Paul Scherrer Institute (Switzerland). The diffractometer was used in high intensity mode ($\Delta d/d \geq 2 \times 10^{-3}$) with a neutron wavelength $\lambda_{neutron} = 0.1494$ nm within the angular 2θ range from 5° to 165°. Quantitative Rietveld refinements of the X-ray and neutron powder diffraction data were performed with the FULLPROF program [17], with the use of its internal tables for scattering lengths and atom form factors.

The as cast $Ti_6Ni_{16}Si_7$ sample was polished using standard procedures and was examined for single-phase condition by optical metallography and scanning electron microscopy (SEM). Compositions were determined via Electron Probe Micro Analyses (EPMA) on a Carl Zeiss DSM 962 equipped with a Link EDX system operated at 20 kV and 60 μA. Binary compounds $TiNi_3$ and $Ni_{31}Si_{12}$ were used as internal EPMA standards.

For DFT calculations we employed the Vienna ab initio simulation package (VASP) [18–20] with the projector augmented wave potential (PAW) [21,22] construction to investigate structural properties and site preferences. An overall energy cutoff of 400 eV was chosen. For the exchange correlation functional the generalized gradient approximation (GGA) of Perdew and Wang [23] was applied. Brillouin zone integrations were performed for suitably large sets of special k points ($5 \times 5 \times 5$) according to Monkhorst and Pack [24]. Optimization of structural parameters (atomic positions and lattice parameters) was achieved by minimization of forces and stress tensors. The accuracy of the calculated total energy is 0.1 meV, i.e. relaxation of the electronic degrees of freedom will be stopped if the total energy change and change of eigenvalues between two steps are both smaller than 0.1 meV.

Enthalpies of formation were derived by the standard procedure shown in our previous publications [25,26] as the difference between the total energy of the considered compounds and the sum of the energies of the

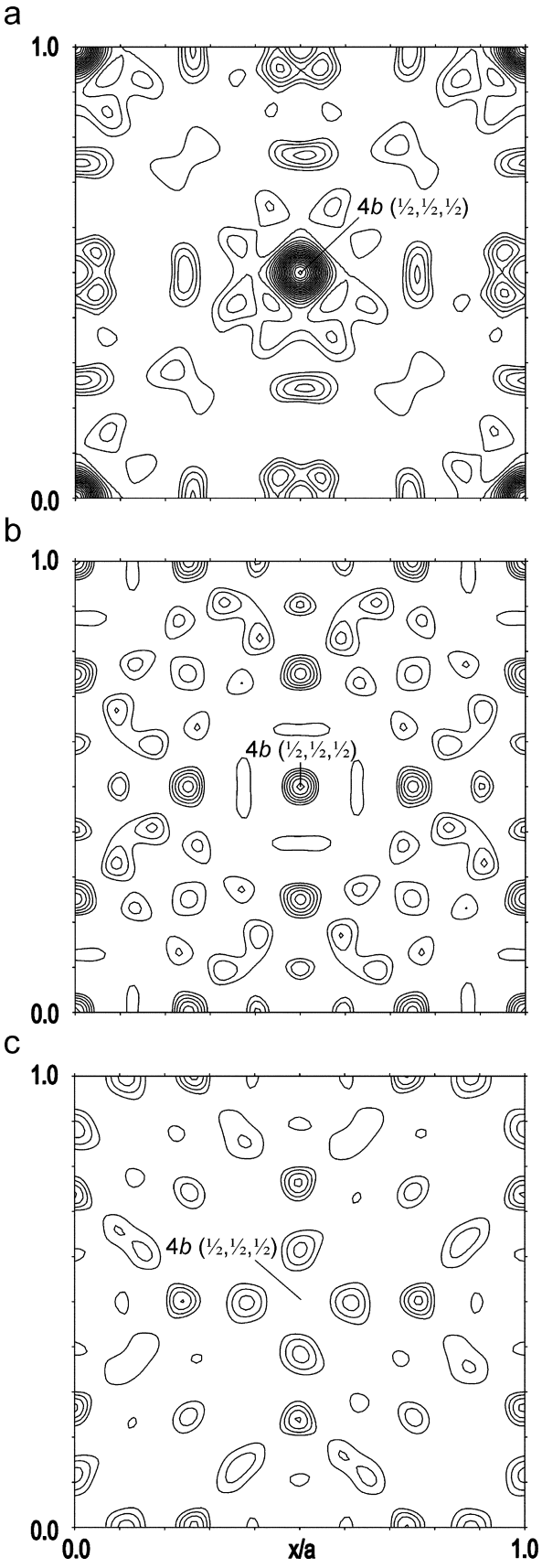

Fig. 1. Fourier difference maps (xy-plane, $z = \frac{1}{2}$; negative electron densities are omitted) for $Ti_6Ni_{16.7}Si_7$ (a), $Zr_6Ni_{16}Si_7$ (b) and $Hf_6Ni_{16}Si_7$ (c) plotted on base of Rietveld refinements of X-ray intensity data ($Mg_6Cu_{16}Si_7$-type space group $Fm\bar{3}m$).

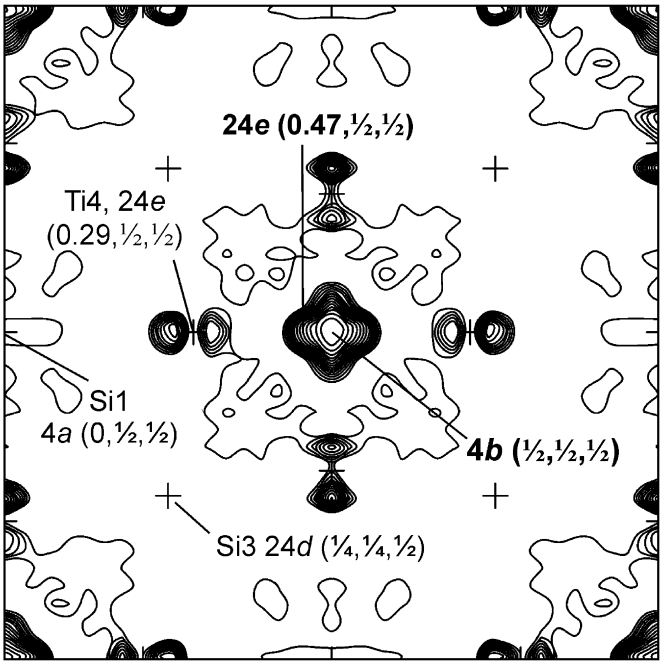

Fig. 2. Fourier difference map (xy-plane, $z=\frac{1}{2}$; negative electron densities are omitted) for $Ti_6Ni_{16.7}Si_7$ plotted on base of refinements of X-ray single crystal data with isotropic ADPs ($Mg_6Cu_{16}Si_7$-type space group $Fm\bar{3}m$). One can see a significant electron density centered in 4*b* $(\frac{1}{2},\frac{1}{2},\frac{1}{2})$ or 24*e* ($x=0.470$, 0, 0) and anisotropy of ADP's for Ti atoms in 24*e* ($x=0.288$, 0, 0).

equilibrium bulk phase of the pure constituents at their specific ground states. Therefore, the equilibrium ground state energies of the pure bulk phases of hcp-Ti, -Zr, and -Hf, ferromagnetic Ni, and diamond Si were calculated in this work.

3. Results and discussion

X-ray powder diffraction intensities recorded from the alloys $M_6Ni_{16}Si_7$ (M = Ti, Zr, Hf) are basically consistent with the cubic Th_6Mn_{23}-type structure (space group $Fm\bar{3}m$). Rietveld refinements of the structures unambiguously located Ni atoms on two 32*f* sites (denoted as *M*5 and *M*6, respectively; see Tables 1 and 2), silicon atoms in the 4*a* and 24*d* positions (*M*1 and *M*3), whilst the 24*e* site hosts the *M* atoms (Ti, Zr, Hf). Fourier maps for $Ti_6Ni_{16}Si_7$ reveal (Fig. 1a), however, additional electron density in the 4*b* site $(\frac{1}{2},\frac{1}{2},\frac{1}{2})$ at an amount of 18 electron/Å^3, whereas no evidence for filling of this site was found for $Hf_6Ni_{16}Si_7$ (Fig. 1c). The residual electron density for $Zr_6Ni_{16}Si_7$ in the 4*b* site $(\frac{1}{2},\frac{1}{2},\frac{1}{2})$ (<3 electron/Å^3) is considered as too small for the presence of an additional atom in the structure. Thus, it appears that only $Ti_6Ni_{16}Si_7$ adopts a filled variant of the Th_6Mn_{23} type, whereas $Zr_6Ni_{16}Si_7$ and $Hf_6Ni_{16}Si_7$ do not contain an additional atom in the 4*b* site. Crystallographic

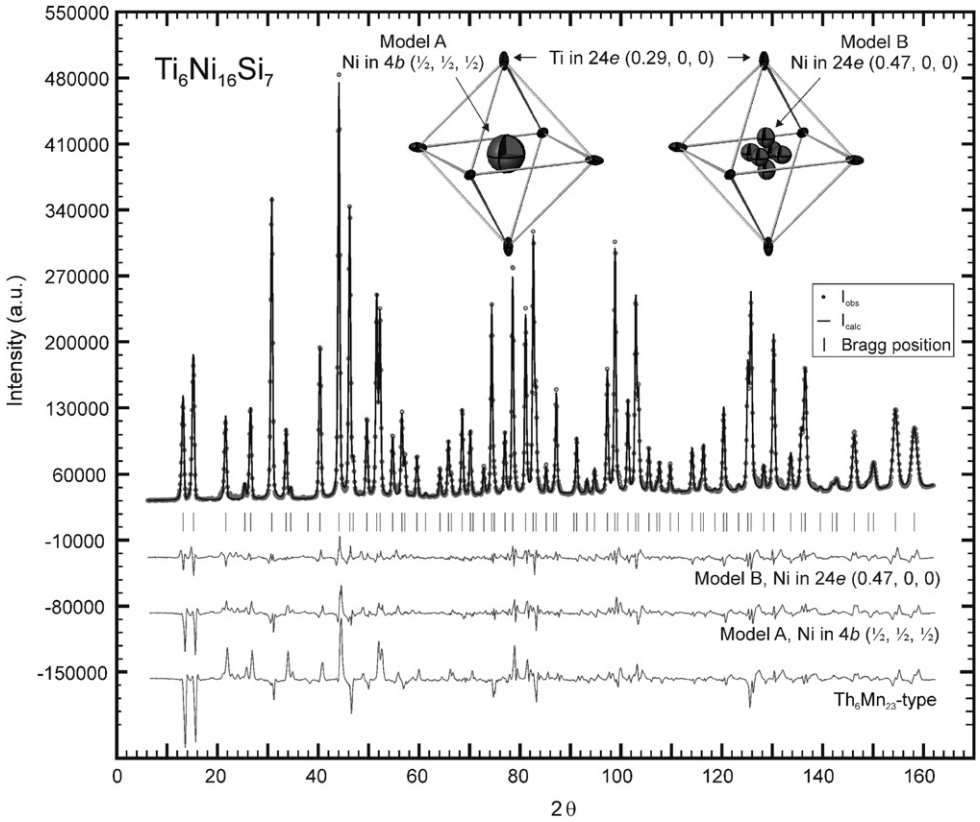

Fig. 3. Results of Rietveld refinement of neutron powder intensity data for $Ti_6Ni_{16.7}Si_7$ (filled variant of the Th_6Mn_{23}-type). I_{calc}–I_{obs} for different models: Th_6Mn_{23}-type, additional atom in the 4*b* site (model A) and additional atom in the 24*e* site (model B).

Table 1
Structural data[a] for the G-phase $Ti_6Ni_{16.43}Si_7$ (EMPA composition Ti21.04Ni54.32Si24.6, space group $Fm\bar{3}m$; No. 225)

Parameter/model	Model A	Model B	Model B	Model C Final structure solution
Formula from refinement (at%)	$Ti_{20.4}Ni_{55.8}Si_{23.8}$	$Ti_{20.2}Ni_{56.3}Si_{23.5}$	$Ti_{20.2}Ni_{56.3}Si_{23.5}$	$Ti_{20.2}Ni_{56.3}Si_{23.5}$
Data collection	Neutron powder diffr.	Neutron powder diffr.	Nonius kappa CCD single crystal	Nonius kappaCCD
Radiation	$\lambda = 0.14940$ nm	$\lambda = 0.14940$ nm	Mo$K\alpha$	Mo$K\alpha$
a (nm) (Guinier)	1.12595(2)	1.12595(2)	1.12595(2)	1.12595(2)
2θ range	$6 \leqslant 2\theta \leqslant 162$	$6 \leqslant 2\theta \leqslant 162$	$4 \leqslant 2\theta \leqslant 70$	$4 \leqslant 2\theta \leqslant 70$
Reflections in refinement	122	122	$208 \geqslant 4\sigma(F_o)$ of 217 (total 1253)	$208 \geqslant 4\sigma(F_o)$ of 217 (total 1253)
Number of variables	25	26	19	22
$R_F = \Sigma\|F_o - F_c\|/\Sigma F_o$	0.021	0.021	$R_F^2 = 0.020$	$R_F^2 = 0.014$
$R_I = \Sigma\|I_o - I_c\|/\Sigma I_o$	0.031	0.029	$R_{Int} = 0.068$	$R_{Int} = 0.068$
$R_{wP} = [\Sigma w_i\|y_{oi} - y_{ci}\|^2/\Sigma w_i\|y_{oi}\|^2]^{1/2}$	0.42	0.042	w$R_2 = 0.052$	w$R_2 = 0.035$
$R_P = \Sigma\|y_{oi} - y_{ci}\|/\Sigma\|y_{oi}\|$	0.031	0.030	GOF = 1.074	GOF = 1.104
$R_e = [(N - P + C)/\sum w_i y_{oi}^2)]^{1/2}$	0.004	0.004	Extinction = 0.0011(1)	Extinction = 0.0011(1)
$\chi^2 = (R_{wP}/R_e)^2$	115	113	Mosaicity = 0.55	Mosaicity = 0.55
Si1 ($M1$); 4a (0,0,0), occ.	1.00	1.00	1.00	1.00
$U_{11} = U_{22} = U_{33}$[b]	$U_{iso} = 0.013(1)$[c]	$U_{iso} = 0.013(1)$[c]	0.0062	0.0054(3)
Ni_1 ($M2$)	4b $(\frac{1}{2},\frac{1}{2},\frac{1}{2})$	24e (x,0,0); $x = 0.470(4)$	24e (x,0,0); $x = 0.4633(6)$	24e (x,0,0); $x = 0.4637(3)$
Occ.	0.749(6)	0.122(8)	0.120(3)	0.119(1)
$U_{11} = U_{33}$; U_{22}	$U_{iso} = 0.09(1)$[c]	$U_{iso} = 0.048(5)$[c]	0.0220, 0.029	0.025(2), 0.019(1)
Si2 ($M3$), 24d $(0,\frac{1}{4},\frac{1}{4})$, occ.	1.00	1.00	1.00	1.00
U_{11}; $U_{22} = U_{33}$; U_{23}	$U_{iso} = 0.0044(5)$[c]	$U_{iso} = 0.0046(5)$[c]	0.0043, 0.0056, 0.0003	0.0037(3), 0.0057(2), 0.0002(2)
Ti ($M4$), 24e (x,0,0)	$x = 0.2856(4)$	$x = 0.2873(3)$	$x = 0.2882(2)$	$x = 0.2927(5)$[0.266(2)]
Occ.	1.00 Ti	1.00 Ti	1.00 Ti	0.78(2)[0.21(2)]
$U_{11} = U_{33}$; U_{22}	$U_{iso} = 0.0137(8)$[c]	$U_{iso} = 0.0114(7)$[c]	0.0065, 0.025	0.0061(6), 0.010(1)
Ni_2 ($M5$), 32f (x,x,x)	$x = 0.33436(6)$	$x = 0.33422(5)$	$x = 0.33426(3)$	$x = 0.33423(2)$
Occ.	1.00	1.00	1.00	1.00
$U_{11} = U_{22} = U_{33}$; $U_{12} = U_{13} = U_{23}$	$U_{iso} = 0.0069(2)$[c]	$U_{iso} = 0.0070(2)$[c]	0.0061, −0.0009	0.0059(1), 0.0014(1)
Ni_3 ($M6$), 32f (x,x,x)	$x = 0.11817(6)$	$x = 0.11828(5)$	$x = 0.11834(3)$	$x = 0.11834(2)$
Occ.	1.00	1.00	1.00	1.00
$U_{11} = U_{22} = U_{33}$; $U_{12} = U_{13} = U_{23}$	$U_{iso} = 0.0080(1)$[c]	$U_{iso} = 0.0067(1)$[c]	0.0062, 0.0014	0.0057(1), −0.0008(1)
Residual electron density; max; min in electrons/nm^3 × 1000	—	—	2.6; −2.7	0.81; −0.70
Intermatomic distances (nm), standard deviations are less than 0.0005 nm				
Si_1($M1$)–8Ni_3	0.2304	0.2307	0.2308	0.2308
–6Ti	0.3206	0.3235	0.3245	0.3296[0.2995]
$M2$–	—	–4Si_2: 0.0478[d] –Si_2: 0.0676[d]	0.0584[d] 0.0826[d]	0.0578[d] 0.0817[d]
–6Ti	0.2414	–1Ti: 0.2057 –4Ti: 0.2419 –1Ti: 0.2733	0.1971 0.2420 0.2898	0.1925[e][0.2226] 0.2370[0.2666] 0.2743[0.3043]
–8Ni_2	0.3230	–4Ti: 0.3050 –4Ti: 0.3439	0.3012 0.3484	0.3015 0.3485
Si_2($M3$)–4Ni_2	0.2298	0.2298	0.2298	0.2298
–4Ni_3	0.2485	0.2484	0.2484	0.2484
–4Ti	0.2843	0.2846	0.2847	0.2856[0.2821]
Ti($M4$)–1$M2$	0.2414	–1Si_2: 0.2057 –4Si_2: 0.2419 –1Si_2: 0.2733	0.1917 0.2420 0.2798	0.1925[0.2226] 0.2370[0.2666] 0.2743[0.2995]
–4Ni_3	0.2663	0.2677	0.2685	0.2721[0.2513]
–4Ni_2	0.2694	0.2692	0.2690	0.2681[0.2749]
–4Si_2	0.2843	0.2846	0.2847	0.2856[0.2821]
Ni5($M5$)–3Si_2	0.2298	0.2298	0.2298	0.2298
–3Ni_3	0.2549	0.2546	0.2546	0.2545
–3Ni_2	0.2686	0.2682	0.2683	0.2682

Table 1 (*continued*)

Parameter/model	Model A	Model B	Model B	Model C Final structure solution
–3Ti	0.2694	0.2692	0.2690	0.2628[0.2749]
$-1Ni_1$	0.3230	$-3Si_2$: 0.3050	0.3012	0.3015
		$-3Si_2$: 0.3439	0.3487	0.3485
$Ni_6(M6)$–$1Si_1$	0.2304	0.2307	0.2308	0.2308
$-3Si_2$	0.2485	0.2484	0.2484	0.2484
$-3Ni_2$	0.2649	0.2546	0.2546	0.2545
–3Ti	0.2663	0.2677	0.2685	0.2721[0.2513]
$-3Ni_3$	0.2661	0.2663	0.2665	0.2665

[a]Crystal structure data are standardized using the program structure tidy [28].
[b]Anisotropic atomic displacement parameters U_{ij} in $10^2\,nm^2$.
[c]Isotropic atomic displacement parameters U_{iso} in $10^2\,nm^2$.
[d]These short distances will not exist in the real structure due to steric reasons.
[e]Value in square bracket correspond to second (split) position of *M*4.

parameters for $Zr_6Ni_{16}Si_7$ and $Hf_6Ni_{16}Si_7$ (unfilled ordered Th_6Mn_{23}-type≡$Mg_6Cu_{16}Si_7$ type) obtained from Rietveld refinements of X-ray and neutron powder diffraction data are available from Table 2. The forthcoming discussion concerns details of the crystal structure of $Ti_6Ni_{16}Si_7$.

Due to the negative neutron scattering length of natural Ti, neutron powder diffraction data are very sensitive to the location of Ti atoms in the crystal structure. Indeed, the neutron data for $Ti_6Ni_{16}Si_7$ reject any Ti atom in the 4*b* site, however, confirm Ti atoms in 24*e* (M4; ($x = 0.287$, 0, 0)). The combined Rietveld refinement of X-ray and neutron powder diffraction data with an additional Si atom in the 4*b* site reveals almost complete occupancy of this site. But atomic displacement parameters (ADP) for atoms in this site were found to be about 3 times higher than those for atoms in other sites of the lattice. As strong correlations between occupancy and ADP in case of powder diffraction data prevent a conclusive determination of atom type and level of filling for this site, X-ray single crystal data were employed for $Ti_6Ni_{16}Si_7$. These data clearly show a significant electron density (~20 electron/Å^3) centered at the 4*b* site (Fig. 2), that can be interpreted either as an additional atom in the 4*b* site $(\frac{1}{2},\frac{1}{2},\frac{1}{2})$ or as a superposition of the electron densities from atoms located in a 24*e* site ($x = 0.470$, 0, 0). Accordingly, we were prompted to consider two possible crystallographic models for $Ti_6Ni_{16}Si_7$ with respect to the mode of filling the $Mg_6Cu_{16}Si_7$-type structure by an additional atom *M*2 (Si or Ni or random mixture of both): (i) *M*2 in the 4*b* site (model A) or (ii) *M*2 in the 24*e* site (model B). Both models after X-ray single crystal and neutron powder diffraction refinement yield very close reliability factors, but model B results in a considerably better fit for the neutron diffraction data at low diffraction angles (Fig. 3). High ADPs are obtained for the filler atoms (*M*2) as well as for their closest neighbors: i.e. the Ti atoms in the *M*4(24*e*) site, which form an octahedron [6*M*4] around the *M*2 atoms. High anisotropy of ADP for Ti atoms is well indicated as residual electron density around the *M*4 site in Fig. 2 (*xy* plane, $z = \frac{1}{2}$, isotropic ADPs for all atoms). This observation, compared with the rather short distances for *M*2–6*M*4 bonds (0.1971 nm, Model B, Table 1), prompts us to consider a possible split of the *M*4 site (model C, Table 1) similar to the G-phase $Ti_{22.5}Ni_{24.5}Al_{53}$ [4]. This model reveals a better fit of single crystal intensities and more reliable interatomic distances, and is therefore accepted as the final structure solution (Table 1).

With respect to the low filling level, both X-ray single crystal and neutron diffraction refinements were unable to distinguish between Ni and Si atoms located in the *M*2(24*e*) site. Refinements reveal very similar reliability factors differing only in the partial occupancy of the *M*2(24*e*) site (2.9 atoms of Ni or 5.9 atoms of Si i.e. 0.7 Ni atoms or 1.5 Si atoms per octahedron, respectively). Nickel atoms seem to be more realistic candidates to occupy the *M*2 site because of three arguments: (i) EPMA data ($Ti_{21.0}Ni_{54.3}Si_{24.7}$ at%) agree better with composition $Ti_{20.2}Ni_{56.3}Si_{23.5}$ (Ni in *M*2) than with $Ti_{19.7}Ni_{52.5}Si_{27.8}$ (Si in *M*2); (ii) the composition $Ti_{19.7}Ni_{52.5}Si_{27.8}$ (Si in the M2) lies beyond the single phase region of the G-phase at 1100 °C (see [13]), and (iii) the octahedra 6*M*4 formed by Ti atoms offer a rather small volume to host more than one Si atom per octahedron. The latter argument follows from a comparison of distances $d_{4b\text{-}M4} = 0.2385$ nm (from the center of the *M*4 octahedron = site 4*b*) to Ti (*M*4) atoms) with the shortest bonds observed in corresponding binary compounds ranging from 0.25 to 0.26 nm [27]. In the final structure solution, the electron density around the center of the *M*4 octahedron is smeared out over Ni atoms partially occupying a 24*e* site (occupancy = 12%) in form of a small octahedron, i.e. the Ni atoms (*M*2) are found in off-center positions (about 0.03 nm from site 4*b*) at an amount of 0.7 Ni per *M*4 octahedron with asymmetric distances $d_{Ni24e\text{–}TiM4}$ ranging from 0.2226 to 0.2743 nm (Table 1). The short distance only allows partial occupation. Accepting Ni atoms for the *M*2 site finally yields the chemical formula $Ti_6Ni_{16.7}Si_7$. Interatomic distances, Ni–Si (*M*1–*M*6, *M*3–*M*5 and *M*3–*M*6) in Table 1 agree well with

Table 2
Structural data[a] for the G-phase in the ternary (Zr, Hf)–Ni–Si systems. (space group $Fm\bar{3}m$; No. 225)

Parameter/alloy composition	$Zr_6Ni_{16}Si_7$	$Hf_6Ni_{16}Si_7$
Formula from refinement (at%)	$Zr_{20.7}Ni_{55.2}Si_{24.1}$	$Hf_{20.7}Ni_{55.2}Si_{24.1}$
Data collection	Image plate powder diffraction	Neutron powder diffraction
Radiation	Cu$K\alpha$1	$\lambda = 0.14940$ nm
a (nm) (Guinier)	1.14652(2)	1.14053(3)
2θ range	$8 \leqslant 2\theta \leqslant 100$	$6 \leqslant 2\theta \leqslant 154$
Reflections in refinement	64	128
Number of variables	19	19
$R_F = \Sigma\|F_o - F_c\|/\Sigma F_o$	0.056	0.015
$R_I = \Sigma\|I_o - I_c\|/\Sigma I_o$	0.059	0.024
$R_{wP} = [\Sigma w_i\|y_{oi} - y_{ci}\|^2/\Sigma w_i\|y_{oi}\|^2]^{1/2}$	0.143	0.035
$R_P = \Sigma\|y_{oi} - y_{ci}\|/\Sigma\|y_{oi}\|$	0.086	0.025
$R_e = [(N-P+C)/\Sigma w_i y_{oi}^2)]^{1/2}$	0.021	0.008
$\chi^2 = (R_{wP}/R_e)^2$	32.4	18.4
Si_1 ($M1$)	4a (0,0,0)	4a (0,0,0)
U_{iso}, occ	0.013(1)[b]; 1.00	0.0042(8)[b]; 1.00
V ($M2$), V = vacancy	4b $(\frac{1}{2},\frac{1}{2},\frac{1}{2})$	4b $(\frac{1}{2},\frac{1}{2},\frac{1}{2})$
Si2 ($M3$), 24d $(0,\frac{1}{4},\frac{1}{4})$	1.00	1.00
U_{iso}, occ.	$U_{iso} = 0.0089(10)$[b]; 1.00	$U_{iso} = 0.0029(4)$[b]; 1.00
$M4$ 24e (x,0,0)	$x = 0.29298(8)$	$X = 0.2943(1)$
U_{iso}	0.0057(6)[b]	0.0020(2)[b]
occ.	1.00 Zr	1.00 Hf
Ni_1 ($M5$), 32f (x,x,x)	$x = 0.33076(7)$	$X = 0.33150(4)$
U_{iso}, occ.	0.0053(4)[b], 1.00	0.0029(1)[b], 1.00
Ni_2 ($M6$), 32f (x,x,x)	$x = 0.11819(7)$	$X = 0.11813(4)$
U_{iso}, occ.	0.0074(3)[b], 1.00	0.0033(1)[b], 1.00
Intermatomic distances (nm), standard deviations are less than 0.0005 nm		
Si_1($M2$)–8Ni_2	0.2347	0.2334
–6$M4$:	0.3359	0.3356
M2–6$M4$	0.2373	0.2346
–8Ni_1	0.3361	0.3329
Si_2 ($M3$)–4Ni_1	0.2341	0.2328
–4Ni_2	0.2531	0.2518
–4$M4$	0.2908	0.2896
$M4$–1V	0.2373	0.2346
–4Ni_2	0.2773	0.2769
–4Ni_1	0.2778	0.2751
–4Si_2	0.2908	0.2896
Ni_1($M5$)–3Si_2	0.2341	0.2328
–3Ni_2	0.2574	0.2565
–3Ni_1	0.2619	0.2629
–3$M4$	0.2778	0.2751
–1V	0.3361	0.3329
Ni_2($M6$)–1Si_1	0.2347	0.2334
–3Si_2	0.2530	0.2518
–3Ni_1:	0.2574	0.2565
–3$M4$	0.2773	0.2769
–3Ni_2	0.2710	0.2695

[a]Crystal structure data are standardized using the program structure tidy [28].[b]isotropic atomic displacement parameters U_{iso} in 10^2 nm^2.

those observed in binary structures i.e. 0.2217 nm for NiSi, 0.2320 for Ni_2Si and 0.2330 for $NiSi_2$ [27]). Interestingly, there are no Ti–Si next nearest neighbor interactions.

In order to check the possibility of a Jahn–Teller like distortion, X-ray single crystal data for $Ti_6Ni_{16.7}Si_7$ were collected in triclinic setting ($a = b = c = 0.79617$ nm, $\alpha = \beta = \gamma = 60^\circ$). A corresponding difference Fourier map F_{obs}–$F_{calc\text{-}M2}$, was calculated for space group $P1$ ($a = b = c = 1.12595$ nm, $\alpha = \beta = \gamma = 90^\circ$, keeping all 116 atoms (except $M2$) fixed at positions known from the cubic setting. The residual electron density located around the $M2$ site clearly showed a superposition of six atoms in form of an octahedron. The shape of the electron density is very similar to that calculated for X-ray single crystal diffraction intensities in cubic symmetry (Fig. 2) and it is without significant tetragonal distortions.

It has to be mentioned that enhanced ADP's for $M2[M4]_6$ atoms were generally observed in the G-phases from the Ti–M–Al systems (M is a transition element of the 8th group, [4–7]), and notably the G-phase $Ti_{22.5}Ni_{24.5}Al_{53}$

shows a split $M4$ site [4]. With respect to the fact that the observed split of the $M4$ site in $Ti_6Ni_{16.7}Si_7$ is certainly associated with the off center position of the $M2$ atom located inside of the $M4$ octahedron, we revisited the shape of the electron density of $M2$ atoms for all the previously investigated Al containing G-phases Ti–{Fe,Co,Ni,Ru, Rh,Os,Ir,Pt}–Al [4–7]. In all these cases, the difference Fourier map ensured a spherical electron density for atoms located in the $M2$ site. As this is also true for the Ti–Ni–Al G-phase with the split Ti-position, the structure of $Ti_6Ni_{16.7}Si_7$ is a unique case among G-phases.

4. Density functional theory calculations

To clarify whether the center of the $[M4]_6$ octahedron (namely, the $M2$ site) is occupied by Ni or Si in the Ti–Ni–Si G (Ti-G) phase and whether $M2$ remains unoccupied in the Zr–Ni–Si (Zr-G) and Hf–Ni–Si G (Hf-G) phases, ab initio DFT calculations were applied for three atomic configurations. For the sake of simplicity, we assume $M2$ in the 4*b* site: (i) Ni in $M2$ (Ni fully occupies the 4*b* site($M2$)); (ii) Si in $M2$ (Si fully occupies the 4*b* site); (iii) vacancy in $M2$ (no atom occupies the 4*b* site). We do not consider configurations where Ti (Zr or Hf) occupies the $M2$ site because diffraction experiments exclude this possibility. Occupation and atom distribution in the remaining sites of the G-phase, namely 4*a*($M1$), 24*d*($M3$), 24*e*($M4$), 32*f*($M5$), and 32*f*($M6$), were taken from experiments (Table 1). Allowing for full geometrical relaxation in the calculation of the total energies, the enthalpies of formation can be obtained by

$$\Delta H(X \text{ in } M2) = E(Z_6Ni_{16}Si_7X) - 7E(\text{Si}) - 16E(\text{Ni}) - 6E(Z) - E(X) \quad (1)$$

in which $E_{(Z6Ni16Si7X)}$, $E_{(\text{Si})}$, $E_{(\text{Ni})}$, $E_{(Z)}$ and $E_{(X)}$ are the calculated total DFT energies at their respective ground states and $Z =$ (Ti, Zr, Hf), and $X =$ (Ni, Si, vacancy). Then, we derive the site preference energy E^{site} as follows:

$$E^{\text{site}}(X \text{ in M2}) = \Delta H(X \text{ in } M2) - \Delta H(\text{vacancy in } M2) = E(X \text{ in } M2) - E(\text{vacancy in } M2) - E(X). \quad (2)$$

Eq. (2) defines the formation enthalpy difference between two competing configurations ((i) and (iii) or (ii) and (iii)) that determine the site preference in the corresponding G-phase (Ni, or Si, or vacancy in 4*b*). If E site (X in $M2$) is negative, the (X in $M2$) configuration is energetically favored over the $M2$ vacancy configuration. In case $E^{\text{site}}(X$ in $M2)$ is positive, the $M2$ vacancy configuration wins out against the (X in $M2$) configuration. If both, E^{site}(Ni in $M2$) and E^{site}(Si in $M2$), are negative, the configuration with the most negative site energy is favored.

For the G-phases of the {Ti,Zr,Hf}–Ni–Si systems, the obtained site energies for (X in $M2$) are plotted in Fig. 4 in comparison to the $M2$ vacancy result. For the Ti-G-phase,

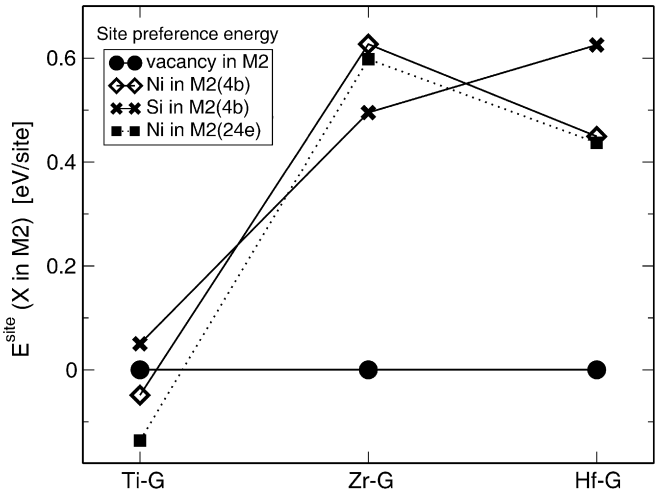

Fig. 4. Calculated site preference energies for the three G-phase series.

Fig. 4 clearly demonstrates, that the site energy $E^{\text{site}}(X$ in $M2)$ is negative for $X =$ Ni, but positive for $X =$ Si confirming the experimental findings (Ni atom in the $M2$ site of "$Ti_6Ni_{17}Si_7$"). However, for the Zr- and Hf-G-phases, site preferences reveal an inverse trend (Fig. 4): the $M2$ vacancy configurations are energetically much more favorable as compared to the (Ni in $M2$) and (Si in $M2$) configurations, which both exhibit considerably positive site energies.

The question therefore arises why Ni prefers the $M2$ site in $Ti_6Ni_{16.7}Si_7$, whereas the $M2$ sites in the Zr and Hf cases are empty. In order to analyze this problem, four model calculations were performed for the (Ni in $M2$) configuration of the Ti-G-phase. For all models initial atomic positions were taken from the calculated (Ni in $M2$) configuration of the Zr-G-phases: (a) all atomic positions are fixed; (b) positions of the Ti atoms ($M4$ site) are relaxed; (c) Ni atoms in $M5$ site are relaxed, (d) Ni atoms in the $M5$ and $M6$ sites are relaxed. These four calculations (a–d) are fixed at the optimized equilibrium volumes of the (Ni in $M2$) cases of the Ti-G-phase. Results in Fig. 5 are compared to the $M2$ vacancy configuration. It has to be noted that the site preference energies for both cases (a) and (b) remain practically unchanged, indicating that Ti atom relaxations have no influence on their site preference energies. However, the relaxation of Ni atoms (models c and d) significantly affects the site preference energy. We clearly see that relaxation of all Ni atoms at the $M5$ and $M6$ sites (case d) results in a stable site configuration, which has almost identical site preference energy with respect to the fully relaxed (Ni in $M2$) configuration of the Ti-G-phase (see Fig. 4). But, relaxation of Ni atoms in the $M5$ site only (case c) is not sufficient. The difference of site preference energies between cases (a) and (d) is about 0.3 eV/site.

Calculations were furthermore used to check for $Ti_6Ni_{17}Si_7$, $Zr_6Ni_{17}Si_7$, $Hf_6Ni_{17}Si_7$ whether (i) Ni atoms occupy the $[M4]_6$ octahedral centers (the 4*b* site) or (ii) Ni

atoms are slightly shifted out of the centers (24*e* site) as shown in diffraction experiments (see above). The 24*e* site in space group $Fm\bar{3}m$ allows for six different positions around the center of each Ti (Zr or Hf) octahedron in form of a small octahedron (see Fig. 3). We hence built six possible configurations, in each of them one Ni atom occupies one of these six positions. The resulting occupation number occ. = 0.16667 is only slightly larger than the experimental value of 0.122. The atom distribution for the remaining sites of the G-phase (4*a*(*M*1), 24*d*(*M*3), 24*e*(*M*4), 32*f*(*M*5), and 32*f*(*M*6)) was taken from the experiment (Table 1). Our calculations found that the six configurations for *M*2 in the 24*e* site yield almost the same total energy with energy differences not exceeding 0.003 eV/unit cell, indicating that Ni atoms may occupy one of the six positions. It is important to note, that for $Ti_6Ni_{17}Si_7$ the site preference energy of Ni in the 24*e* site is about −0.136 eV/site (see Table 3), which is much lower by about 0.08 eV/site than that calculated for Ni in the 4*b* site (Fig. 4) in excellent agreement with the experimental finding. However, for $Zr_6Ni_{17}Si_7$ and $Hf_6Ni_{17}Si_7$ the site preference energies of Ni in the 24*e* site are both positive (0.597 and 0.437 eV), respectively, but just slightly lower than those of Ni in the 4*b* site (Fig. 4). This provides a further convincing evidence that the centers of each Zr and Hf octahedron remain empty, supporting our experimental investigations. Finally, the ab initio results are compared to the experimental parameters in Table 3 from which we see a good agreement. The calculated lattice constants are slightly larger by 1%, and the internal atomic parameters are almost identical with the experimental values. The calculated enthalpies of formation of $Ti_6Ni_{17}Si_7$, $Zr_6Ni_{16}Si_7$, and $Hf_6Ni_{16}Si_7$ are compiled in Table 3.

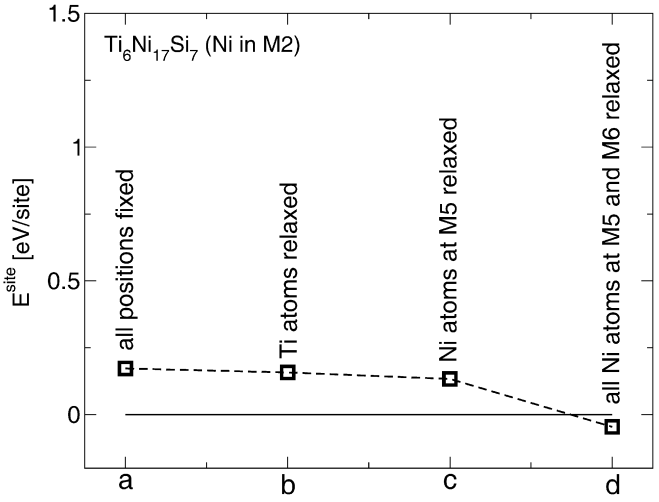

Fig. 5. Calculated site preference energies in four different models (a–d) for the (Ni in *M*2) configuration of the Ti-G-phase by inserting the optimized atomic positions of the (Ni in *M*2) configuration in the Zr-G-phase. For details, see text.

5. Conclusion

X-ray powder/single crystal and neutron powder diffraction data defined an ordered Th_6Mn_{23} type ($Mg_6Cu_{16}Si_7$-type space group $Fm\bar{3}m$) for $M_6Ni_{16}Si_7$ (M = Zr, Hf), whereas $Ti_6Ni_{16.7}Si_7$ is a new variant of the filled Th_6Mn_{23}-type structure containing an additional Ni atom in the 24*e* site (*M*2 site, $x = 0.4637,0,0$; occ. = 0.119) inside a Ti octahedron, where Ti atoms occupy a split position. Ab initio density functional theory calculations confirm that Ni atoms prefer the *M*2 site (24*e*) in $Ti_6Ni_{16.7}Si_7$, whereas the *M*2 sites in the Zr and Hf cases remain vacant. Enthalpies of formation of $Ti_6Ni_{17}Si_7$, $Zr_6Ni_{16}Si_7$, and

Table 3
Comparison between calculated and experimental parameters for the G-phase in the ternary (Ti, Zr, Hf)–Ni–Si system. (space group $Fm\bar{3}m$, No. 225). Note that, *M*2–Ni(24*e*) denotes that Ni occupies the 24*e* site of *M*2

		$Ti_6Ni_{16}Si_7$ vacancy in *M*2	$Ti_6Ni_{17}Si_7$ Ni in *M*2 (4*b*)	$Ti_6Ni_{17}Si_7$ Ni in *M*2 (24*e*)	$Zr_6Ni_{16}Si_7$ vacancy in *M*2-	$Zr_6Ni_{17}Si_7$ Ni in *M*2 (4*b*)	$Hf_6Ni_{16}Si_7$ vacancy in *M*2	$Hf_6Ni_{16}Si_7$ Ni in *M*2 (4*b*)
a (nm)	Calc.	1.11869	1.12726	1.12802	1.14881	1.15912	1.14136	1.14562
	Expt.		1.12595(2)	1.12595	1.14652(2)		1.14053(3)	
M2 4*b*(1/2,1/2,1/2) or 24*e* (*x*,0,0)	Calc.		4*b*: Ni(occ. = 1)	24*e*: Ni(occ. = 0.167) $x = 0.46466$		4*b*: Ni(occ. = 1)		4*b*: Ni(occ. = 1)
	Expt		4*b*: Ni(occ. = 0.429)	24*e*: Ni(occ. = 0.122) $x = 0.46330$				
*M*4 24*e* (*x*,0,0)	Calc.	0.29829	0.28344	0.28279	0.29286	0.28163	0.29425	0.28224
	Expt.		0.2873(3)	0.28820(2)	0.29298(8)		0.29430(1)	
*M*5 (Ni) 32*f*(*x*,*x*,*x*)	Calc.	0.33474	0.33454	0.33623	0.33107	0.33094	0.33215	0.33209
	Expt.		0.33422(5)	0.33426(3)	0.33077(7)		0.33150(4)	
*M*6 (Ni) 32*f*(*x*,*x*,*x*)	Calc.	0.11778	0.11823	0.11776	0.11814	0.11901	0.11807	0.11885
	Expt.		0.11828(5)	0.11834(3)	0.11819(7)		0.11813(4)	
ΔH (kJ/mol at.)	Calc	−68.21	−68.36	−68.65	−74.78	−72.76	−78.59	−77.14
E_{site} *X* in *M*2), eV/site	Calc	0	−0.048	−0.1365	0	0.6269	0	0.4493

$Hf_6Ni_{16}Si_7$ were calculated to be −68.65, −74.78, and −78.59 kJ/(mol of atoms), respectively.

Acknowledgments

The research reported herein was sponsored by the Austrian National Science Foundation FWF under Grants P16957, P16778. This work was partially performed at the spallation neutron source SINQ, Paul Scherrer Institute, Villigen, Switzerland.

References

[1] J.J. Ding, H. Schweiger, W. Wolf, P. Rogl, D. Vogtenhuber, R. Podloucky, in: Gamma Titanium Aluminides 1999, Proceedings of Symposium held during the 1999 TMS Annual Meeting,. TMS—Miner. Metals and Mater. Soc., San Diego, CA, USA, 1999, p. 141.
[2] J.J. Ding, P. Rogl, B. Chevalier, J. Etourneau. Intermetallics 8 (2000) 1377.
[3] J.J. Ding, P. Rogl, H. Schmidt, R. Podloucky, Lvisk. Lvivsk, UN-TU 2000, Ser. Khim. 39C:136.
[4] A. Grytsiv, J.J. Ding, P. Rogl, F. Weill, B. Chevalier, J. Etourneau, G. André, F. Bourée, H. Noël, P. Hundegger, G. Wiesinger, Intermetallics 11 (2003) 351.
[5] A. Grytsiv, P. Rogl, H. Schmidt, G. Giester, P. Hundegger, G. Wiesinger, V. Pomjakushin, Intermetallics 12 (2004) 563.
[6] A. Grytsiv, P. Rogl, G. Giester, V. Pomjakushin, Intermetallics 13 (2005) 497.
[7] A. Grytsiv, P. Rogl, V. Pomjakushin, Intermetallics 14 (2006) 784.
[8] H.J. Beattie Jr., F.L. VerSnyder, Nature 178 (1956) 208.
[9] H.J. Beattie Jr., W.C. Hagel, Trans. AIME 209 (1957) 911.
[10] E.I. Gladyshevskii, P.I. Kripyakevich, Y.u.B. Kuz'ma, T. Myu, Sov. Phys.-Crystallogr. 6 (1961) 615 (Translated from Krystallographiya).
[11] E.I. Gladyshevskii, Sov. Powder Metall. 1 (1962) 262 (Translated from Poroshkovaya Metallurgiya).
[12] F.X. Spiegel, D. Bardos, P.A. Beck, Trans. Metall. Soc. AIME 222 (1963) 575.
[13] X. Hu, G. Chen, C. Ion, K. Ni, J. Phase Equilibria 20 (1999) 508.
[14] Nonius Kappa CCD Program Package COLLECT, DENZO, SCALEPACK, SORTAV, Nonius Delft, The Netherlands, 1998.
[15] G.M. Sheldrick. SHELXL-97, Program for Crystal Structure Refinement. University of Göttingen, Germany; Windows version by McArdle, National University of Ireland, Galway, 1997.
[16] P. Fischer, G. Frey, M. Koch, M. Koennecke, V. Pomjakushin, J. Schefer, R. Thut, N. Schlumpf, R. Buerge, U. Greuter, S. Bondt, E. Berruyer, Physica B 276–278 (2000) 146.
[17] T. Roisnel, J. Rodriguez-Carvajal, Mater. Sci. Forum 378–381 (2001) 118.
[18] G. Kresse, J. Hafner, Phys. Rev. B 48 (1993) 13115.
[19] G. Kresse, J. Furthmueller, Comput. Mater. Sci. 6 (1996) 15.
[20] G. Kresse, J. Furthmueller, Phys. Rev. B 54 (1996) 11169.
[21] P.E. Blöchl, Phys. Rev. B 50 (1994) 17953.
[22] G. Kresse, D. Joubert, Phys. Rev. B 59 (1999) 1758.
[23] J.P. Perdew, Y. Wang, Phys. Rev. B 45 (1992) 13244.
[24] H.J. Monkhorst, J.D. Pack, Phys. Rev. B 13 (1976) 5188.
[25] X.Q. Chen, V.T. Witusiewicz, R. Podloucky, P. Rogl, F. Sommer, Acta Mater. 51 (2003) 1239.
[26] X.Q. Chen, W. Wolf, R. Podloucky, P. Rogl, Phys. Rev. B 71 (2005) 174101.
[27] Pauling File Binary Edition, Version 1.0, Release 2002/1, ASM International, Materials Park, OH, USA.
[28] E. Parthé, L. Gelato, B. Chabot, M. Penzo, K. Cenzual, R. Gladyshevskii, TYPIX Standardized Data and Crystal Chemical Characterization of Inorganic Structure Types, Springer, Berlin, Heidelberg, 1994.